Polymer Journal, Vol. 31, No. 11-1, pp 948—954 (1999)

Effects of Oxygen on Thermal Dehydrochlorination of Poly(vinylidene chloride)

Tar-Hwa HSIEH

Department of Chemical Engineering, National Kaohsiung Institute of Technology, Kaohsiung, Taiwan 80782, Republic of China

(Received April 16, 1999)

ABSTRACT: The early stages of thermal degradation below 1% dehydrochlorination poly(vinylidene chloride) (PVDC), can be divided into an induction period, period with conversion below 0.1% dehydrochlorination, and that with conversion ranging from 0.1 to 1%. The time of induction period increases with oxygen concentration due to retardation effect. The second and third stages of degradation follow the apparent zero-order reaction and rates of dehydrochlorination of both stages increase linearly with oxygen concentration. The melting points of samples with different degrees of degradation show a decreasing trend with degrading time regardless of annealing effect. By combination with our differential scanning calorimetry (DSC) thermograms and wide-angle X-ray diffraction (WAXD) patterns, in the presence of pure oxygen which first reacts with the PVDC dangling chains outside the crystalline, and cuts through the degraded crystalline along the backbones resulting in many pieces of small crystallite. A polarity change of PVDC characterized by solid-state nuclear magnetic resonance (NMR) due to degradation can be observed.

KEY WORDS Poly(vinylidene chloride) / Thermal Degradation / Oxygen Effect / Kinetic Study / Dehydrochlorination /

Due to excellent gas impermeability, oxidation resistance and resistance of biodegradation,[1,2] poly(vinylidene chloride) (PVDC) is an important material for preparation of fiber, latex, and film. However, discoloration, crosslinking, and reduction of the mechanical properties because of the poor thermal stability,[3-5] that easily occur when exposed to heat or light, turn out to be the main problems for storage and processing of the PVDC solid. A great amount of literature[6-32] concerning the thermal dehydrochlorination of PVDC was performed at higher degree of dehydrochlorination with inert gas as the carrier medium. Little attention was paid to correlate the degradation at the early stage of conversion, below 1%, to the effect of oxygen. Dolezel[4] claimed the reaction rate of the dehydrochlorination of PVDC up to 10% conversion, is larger in oxygen than that in air or nitrogen. However, the relationship of the early degradation polymer structure and atmosphere was not carefully studied. Consequently, an understanding of the effects of oxygen on initial thermal degradation of PVDC is extremely important for processing control or stabilization mechanism studies.

PVDC solid starts to degrade at about 120°C and hydrochloride is the only gas product below 190°C.[5-7] Therefore, measuring the amount of evolved hydrochloric gas within this temperature range (120—190°C) is an effective way of studying the early stage of degradation of PVDC.[31] The rate of dehydrochlorination can be accurately measured to a conversion of 10^{-4} %[30,31] by measuring change in pH of the absorbing potassium hydroxide aqueous solution. Using intrinsic viscosity data,[3,34] DSC thermograms,[34] X-ray patterns,[34] and solid-state nuclear magnetic resonance (NMR) spectra, the effects of oxygen on change of molecular structure and crystalline morphology during degradation below 1 % conversion can also be studied.

EXPERIMENTAL

Materials

Name	Source	Grade
Vinylidene chloride	Merck	Extra pure
Ammonium persulfate	Hayashi	Extra pure
Sodium bisulfite	Wako	Extra pure
Sodium lauryl sulfate	Hayashi	Extra pure
Potassium chloride	Shimatsu	Extra pure
Hexamethylene phosphoramide (HMPA)	Aldrich	Extra pure

Preparation of Poly(vinylidene chloride)[35]

A three-necked flask with mechanical stirrer, condenser and inlet of adapter connected to nitrogen gas was used as a reactor. 100 g vinylidene chloride were added to a 100 mL water solution with 1 g sodium lauryl sulfate followed by addition of 0.5 g of ammonium persulfate and 0.5 g sodium bisulfite.

The mixture was turned into an emulsion by stirring and polymerized at a speed of 250 rpm at 26°C. The polymerization continued for 6 h followed by addition of 100—150 mL saturated sodium chloride aqueous solution to precipitate the polymers. The white powders of PVDC were isolated by filtration, purified by washing with distilled water and dried in vacuum oven at 40°C for more than 24 h. The obtained PVDC powder was characterized by an elementary analyzer, Heraeus CHN-rapid and Tacussel Coulomax 78. The results are listed in Table I. Particle size of the samples was controlled by passing through a 250 mesh sieve.

Purification of the Atmosphere[36]

The atmosphere with various oxygen concentrations was prepared from mixing the needed amount of pure oxygen and nitrogen together. The mixture gas was first bubbled through a carbon dioxide absorber of a 50%

Table I. Elementary analysis of emulsion polymerized PVDC

		C	H	Cl
$(CH_2CCl_2)_n(97)_n$	Calcd	25.19	2.68	72.15
	Found	25.13	2.59	72.14

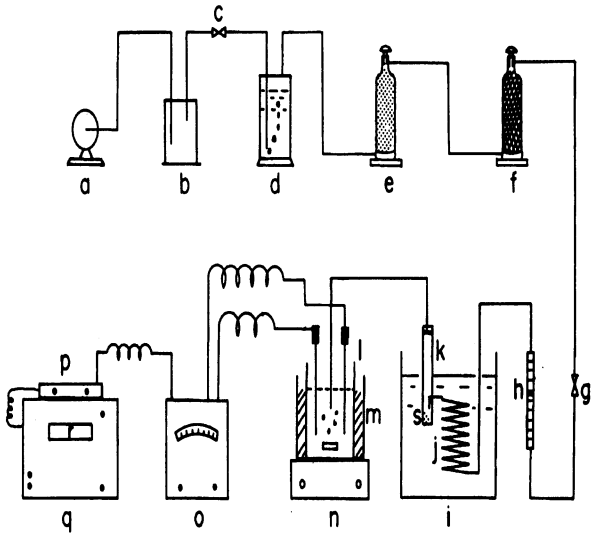

Figure 1. Apparatus for thermal degradation. a, compressor (gas bomb); b, buffer; c, needle valve; d, CO_2 absorber; e, silica gel column; f, dust catcher; g, needle valve; h, flow meter; i, thermostat; j, glass heating coil; k, reaction vessel; l, pH measuring cell; m, cooling unit; n, magnetic stirrer; o, pH meter; p, EPR pre-box; q, recorder; s, sample.

aqueous solution of potassium hydroxide. The gas was then dried and dust removed in a dust collector and preheated to the reaction temperature before going into the reaction vessel. The thermal degradation apparatus is shown in Figure 1.

Oxygen free nitrogen gas was obtained by purging the neat nitrogen gas through pyragallol hydroxide aqueous solution before going into the carbon dioxide absorber. Different oxygen concentration mixtures can be obtained by mixing necessary amounts of purified nitrogen with carbon dioxide free oxygen gas.

Measurement of the Degree of Dehydrochlorination of PVDC[30,31,37]

The heating coil and reaction vessel for thermal degradation studies is shown in Figure 2. 0.2 g PVDC powder was added to the reactor kept at constant temperature (170, 180, and 190°C) in a silicone oil bath. A purified gas with different oxygen concentration was purged through the reactor at 6.28 L h^{-1} and the resulting HCl gas was purged by the atmosphere and placed in a stirred 60 mL 0.1 *N* KOH aqueous solution. pH of the KOH aqueous solution was measured with time.

Preparation of Samples with Different Conversion

When pH reached the given conversion, the reactor was taken from the oil bath and quenched in a dry ice bath in order to stop further degradation. Cooled samples with different conversions were isolated and dried in a vacuum oven controlled at room temperature.

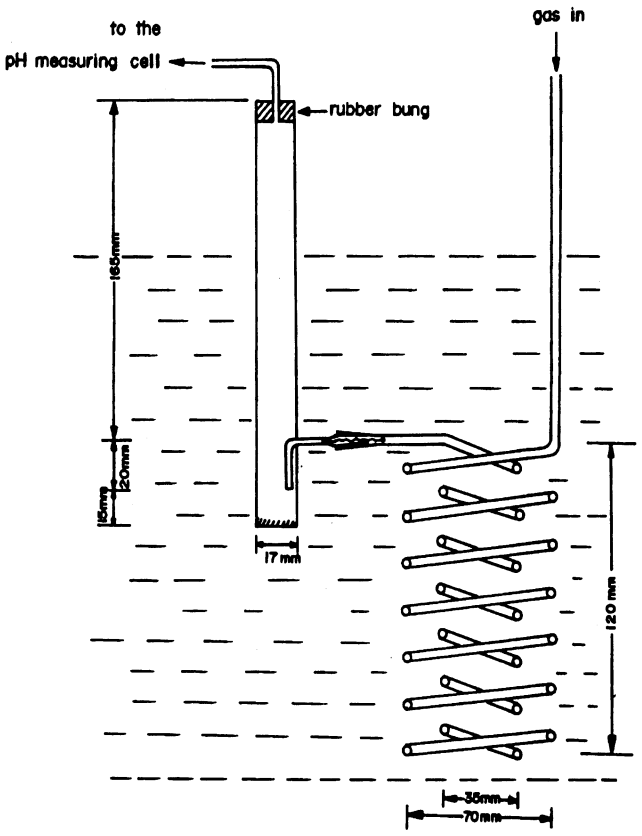

Figure 2. Heating coil and reaction vessel for thermal degradation.

Intrinsic Viscosity $[\eta]$[33]

The purified and dried samples were dissolved in HMPA. $[\eta]$ was measured by an Ubbelohde viscometer in a water bath kept at 25 ± 0.1°C and an average viscosity molecular weight of 4.3×10^4 was obtained by the equation $[\eta] = 2.58 \times 10^{-4} M^{0.65}$.

Differential Scanning Calorimetry (DSC) Thermogram

DSC thermograms of the samples were performed by a Perkin-Elmer-7 series at a heating rate of 40°C min^{-1} from 100 to 250°C. At this heating rate temperature range, the rate of dehydrochlorination of samples may be negligible. The peak position of the heat absorption region is defined here as melting point. The purging gas was nitrogen at a flow rate of 10 mL min^{-1}. Calibration of the calorimeter was conducted for this heating rate using indium standard.

X-Ray Diffraction Patterns

The X-ray diffraction patterns of samples were obtained from exposure to a Siemen D5000 X-ray source with Cu-K_α (1.542A) as target. The diffraction angles (2θ) ranged from 2 to 40 degree with a power of 40 kV and 30 mA.

Solid-State NMR (Nuclear Magnetic Resonance)

The degraded PVDC powder was analyzed by a Bruker DSX 400 NMR with CP/MAS probe and magnetic field source of 400 MHz.

Table II. Time of each stage at 180°C at various percentages of oxygen

Period of time / min	0% (Nitrogen)	21% (Air)	50%	100% (Oxygen)
1st	0—11	0—18	0—24	0—39
2nd	11—13	18—19	24—25	39—40
3rd	13—18	19—27	25—31	40—44

Table III. Time of each stage at 190°C at various percentages of oxygen

Period of time / min	0% (Nitrogen)	21% (Air)	50%	100% (Oxygen)
1st	0—10.2	0—11	0—11.2	0—12
2nd	10.2—11.2	11—11.8	11.2—12.2	12—13
3rd	11.2—14.6	11.8—15.5	12.2—16	13—16.6

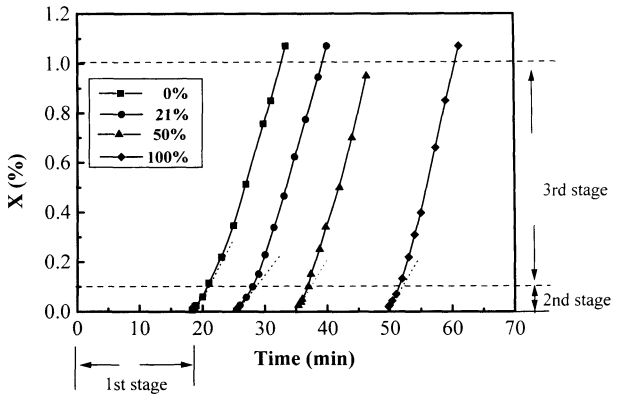

Figure 3. Diagram of conversion *vs.* degradation time at various oxygen concentrations at 170°C.

RESULTS AND DISCUSSION

Kinetic Studies

The early stages of thermal degradation below 1% dehydrochlorination of PVDC may be divided into an induction period, period below 0.1% dehydrochlorination and conversion ranging from 0.1 to 1%. The diagrams of dehydrochlorination reaction below 1% subject to different oxygen concentration are shown in Figure 3. The time period consumed at each stage at various concentrations of oxygen at a given temperature is illustrated in Tables II to III. In Figure 3 and Tables II to III, the period time of the first stage is dependent on type of environment gas and degradation temperature. Thermal degradation in oxygen environment has the longest induction period. The shortest period is degradation under nitrogen gas at higher temperature. Two possible mechanisms contribute to increase of the induction period when degradation is performed in pure oxygen.[37] One is the formation of peroxide radical resulting from the reaction of alkyl radical with oxygen to retard dehydrochlorination, as shown in Scheme 1 (*cf.* type 1). Another retardation effect is the formation of the chlorinated epoxide groups originated from opening the insertion into the double bonds by oxidation at the chain ends. The oxirane groups break later on and produce the alkoxy radicals, which initiate thermal degradation, as demonstrated in Scheme 1 (*cf.* type 2). Until enough evolved hydrochloride gas is produced, the thermal degradation goes to the second stage, and we can detect the presence HCl gas by the change of the pH of KOH aqueous solution. At high temperature (190°C), these oxygen retardation effects from pure oxygen decrease rapidly and reduce induction time. This implies that peroxide groups break more easily and quickly at higher temperature, to compensate for the retardation effect of oxygen and shortens the induction time. However, in an air stream, only 21% oxygen, the effect of oxygen is not significant compared to pure oxygen. A nitrogen environment, which has no oxygen, demonstrates the least oxygen retardation effect. The quantitative effects of oxygen concentration on the rate of dehydrochlorination is given in Figure 4.

As shown in Figure 4, good linear relationship between oxygen concentration and rate of dehydrochlorination at the second stage is observable. Similar dehydrochlorination behavior was found for the third stage. The rate of dehydrochlorination increases linearly with oxygen concentration and is expressed as:

$$R_d = B + CY \quad (1)$$

Where R_d is the rate of dehydrochlorination, B and C are constants, and Y is the volume fraction of oxygen in the mixed atmosphere. B and C obtained from at different degradation temperatures are listed in Table IV that illustrates increase with temperature, revealing that degradation temperature has significant effect on initial degradation. For the third stage of degradation, however, this tendency is more significant.

The rate of early degradation of PVDC can be expressed as:

$$R_d = dX/dt = kf(X) = A\exp(-E_a/RT)f(x) \quad (2)$$

Where X is the conversion defined as the ratio of the produced HCl to that of the theoretical HCl amount at 100% dehydrochlorination, k is the rate constant, $f(x)$ is function of conversion, A is the frequency factor, E_a is the apparent activation energy, R is the gas constant, and T is absolute temperature.

For an nth-order reaction, *i.e.*, $f(X) = (1-X)^n$, where n is the reaction order. Equation 2 can be rewritten as:

$$R_d = A\exp(-E_a/RT)(1-X)^n \quad (3)$$

If the thermal dehydrochloranation follow a zero order reaction. Equation 3 becomes:

$$R_d = A\exp(-E_a/RT) \quad (4)$$

As illustrated in Figure 5, good linear relationship between $\ln R_d$ and reciprocal temperature is observed. The apparent activation energy of the second and third stages can be obtained from the slopes of the curves in Figure 5. E_a are given in Table V showing the increasing apparent activation energy of the second stage with oxygen concentration and slight decrease for the third one. These results are consistent with the previous study,[37] that derived a zero order reaction for dehydrochlorination in the second and third stages.

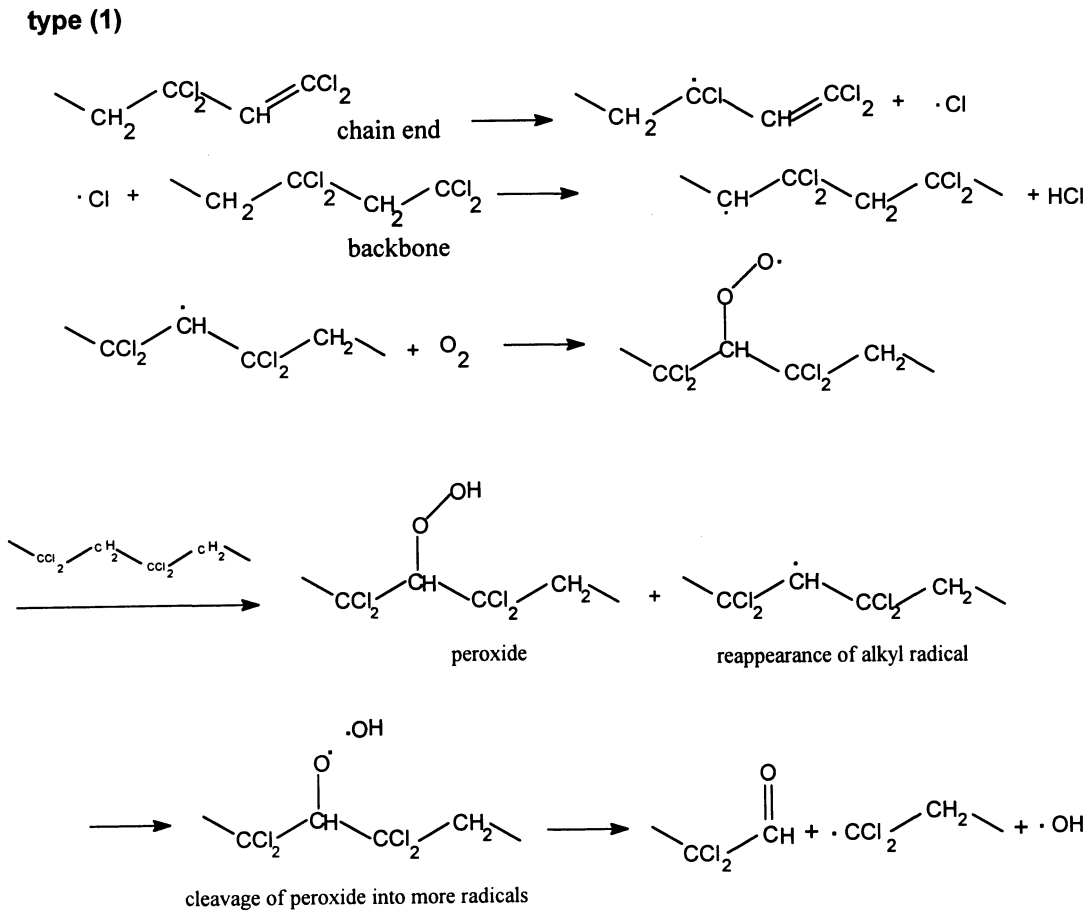

Scheme 1. Retardation effect of oxygen.

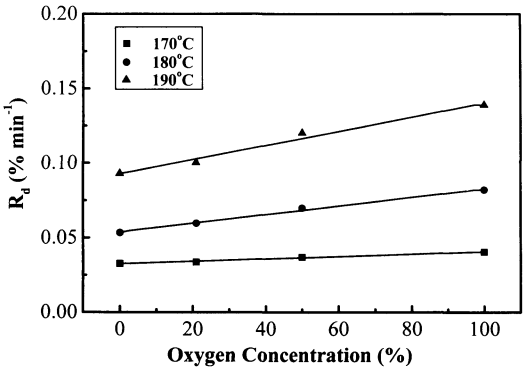

Figure 4. Diagram of rate of dehydrochlorination *vs.* oxygen concentration for PVDC at the second stage.

Table IV. Values of B and C obtained from eq 1

	Stage number			
	Second		Third	
Temperature/°C	$B \times 10^{-2}$	$C \times 10^{-2}$	$B \times 10^{-2}$	$C \times 10^{-2}$
170	3.24	7.99	7.92	26.31
180	5.39	28.89	13.62	45.96
190	9.26	47.48	22.12	47.95

Differential Scanning Calorimetry

Figure 6 shows the melting point depression of PVDC solid with increasing oxygen concentration by DSC thermograms. The presence of oxygen gas accelerates the degradation at the crystalline region.[5] The degraded crystalline region creates a low barrier since most of the gas cannot penetrate denser neat crystalline region of PVDC. The degradation causes melting point depression as seen in Table VI at various oxygen concentrations. However, the melting point, which related to the degraded or non-degraded crystalline region, depends on competition between degradation and annealing effects. If degradation is not present at such high temperature,

Table V. Apparent activation energy of second and third stages of dehydrochlorination reaction at different oxygen percentages

Oxygen concentration/%	0		21		50		100	
Stage number	2nd	3rd	2nd	3rd	2nd	3rd	2nd	3rd
Apparent activation energy E_a/kcal mol^{-1}	21.6	21.9	22.6	21.6	24.2	21.4	25.4	16.9

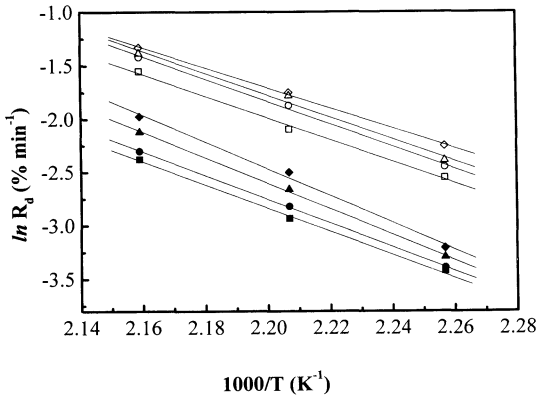

Figure 5. Arrhenius diagrams for second and third stages of thermal degradation of PVDC at various oxygen concentrations. Second stage: (■), 0% ; (●), 20%; (▲), 50% ; (◆), 100%. Third stage: (□), 0% ; (○), 20% ; (△), 50% ; (◇), 100%.

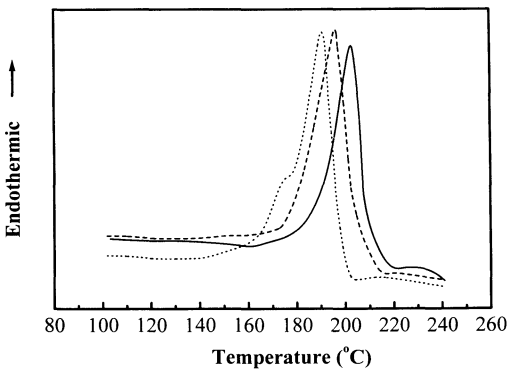

Figure 6. DSC thermograms of PVDC treated in various atmospheres. (—), N_2; (---), Air; (...), O_2.

the melting point goes higher due to the annealing effect and increase the lamella thickness, which would make the sample become denser and improves the capacity as a gas barrier.

The viscosity increases much faster than the depression of melting point with oxygen concentration according to Table VI. This implies the thermal degradation results in more crosslinking and less chain-scission of the backbones. The melting point is depressed after crosslinking due to reduce the ability to crystallize.

Wide-Angle X-Ray Diffraction Patterns

Wide-angle X-ray diffraction (WAXD) patterns were used to analyze the degradation of PVDC solid in different purging gas containing various oxygen concentrations. In the beginning, PVDC annealed at 170°C in nitrogen environment is exposed to X-ray and the diffraction patterns at various annealing times are shown in Figure 7. Even though, there is already 0.1% dehydrochlorination which takes 21 min as shown in Figure 3, no significant change of crystalline lattice as seen in Figure 7 due to the inertness of nitrogen gas.

When air is used as the environment gas, the WAXD data show a similar pattern with that in nitrogen as seen in Figure 8. The incorporation of 21% oxygen in the purging gas does not show a different diffraction pattern with that in pure nitrogen.

A different WAXD pattern is found when PVDC solid is subjected to pure oxygen gas during degradation. Figure 9 shows a large peak at about 12° for 60 min annealing in pure oxygen. The big domain appearing at the smaller angle is considered the product obtained from oxidation and dehydrochlorination. Dehydrochlorination proceeds through the crystalline region would happen if the crystal surface is undergoing degradation.[5] Oxygen gas first reacts with dangling unsaturated chain ends outside the crystal then follow the unzipping dehydrochlorination reaction into the crystals and cut the crystalline into many pieces. These pieces of crystals create an absorption peak at the lower angle in longer annealing time as shown in Figure 9, which is similar to the formation of mosaic structure.[38]

Less degraded or non-degraded crystalline grows due to annealing, which can be confirmed form the shaper peaks at higher angles. At higher temperature, the cleavage of crystalline region from dehydrochlorination is accelerated due to the presence of more active oxygen molecules as seen from Figure 10. For 180 and 190°C,

Table VI. Effects of oxygen concentration on melting point and intrinsic viscosity of PVDC at 170°C

Oxygen concentration/%	0		21		50		100	
Conversion/%	T_m	$[\eta]$	T_m	$[\eta]$	T_m	$[\eta]$	T_m	$[\eta]$
	°C	dL g^{-1}	°C	dL g^{-1}	°C	dL g^{-1}	°C	dL g^{-1}
0	200	0.26	200	0.26	200	0.26	200	0.26
0.025	199	0.37	199	0.55	199	0.56	199	0.69
0.05	198	0.47	198	0.56	198	0.70	197	0.72
0.10	198	0.5	198	0.63	197	0.73	196	0.75
1.00	196	—[a]	196	—[a]	195	—[a]	195	—[a]

[a] Insoluble.

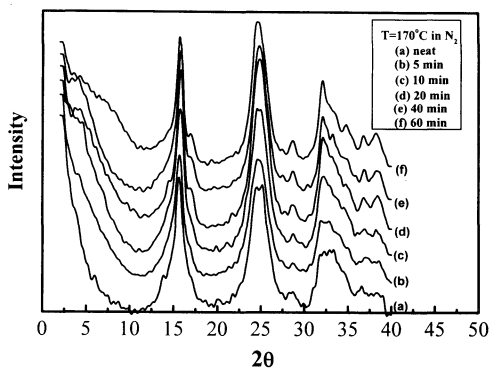

Figure 7. X-Ray diffraction patterns of PVDC solid taken in N_2 at 170°C.

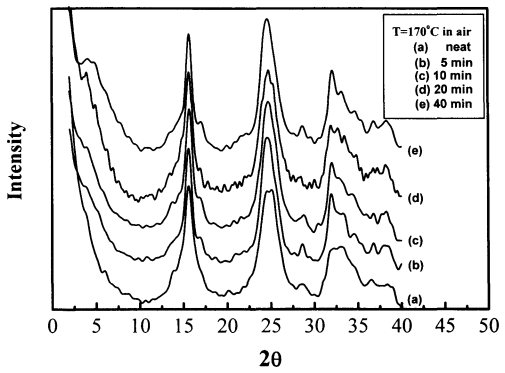

Figure 8. X-Ray diffraction patterns of PVDC taken in air at 170°C.

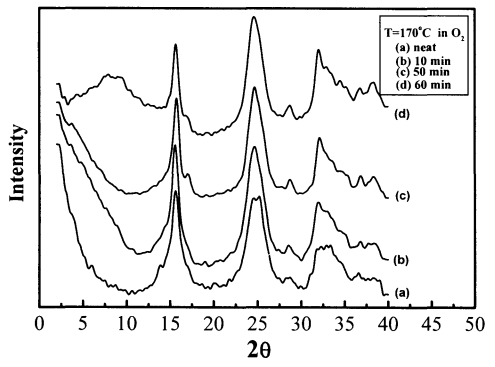

Figure 9. X-Ray diffraction patterns of PVDC solid annealed in pure O_2 at 170°C.

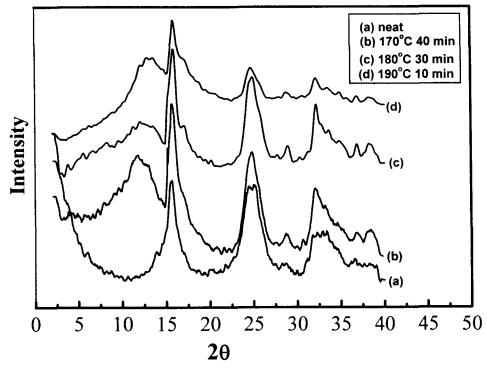

Figure 10. X-Ray diffraction patterns at various temperatures and annealing time.

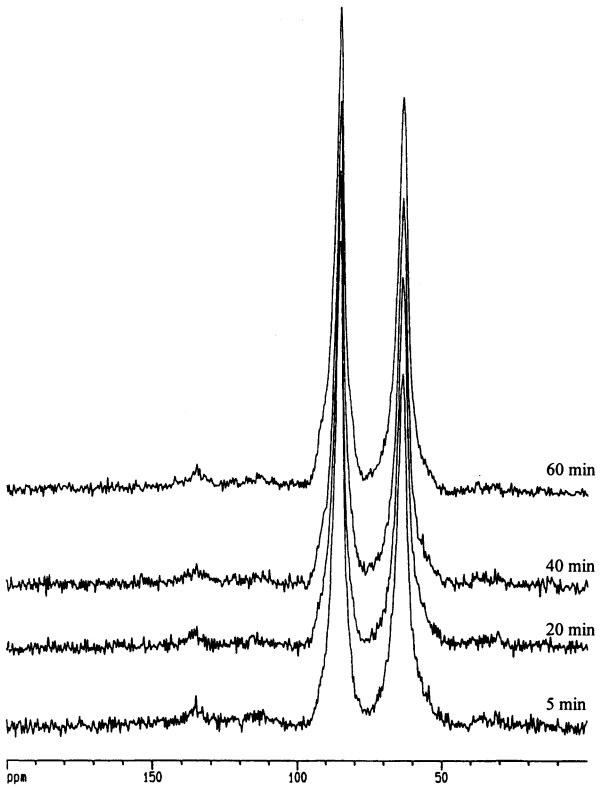

Figure 11. ^{13}C solid-state NMR spectra of PVDC annealing for various times at 170°C in air.

the lower angle peak appears earlier at the same angles as that at 170°C and the size is about the same that at 170°C (6.6 A). The presence of the big domain is believed to be caused from oxidation and degradation.[38]

Solid-State NMR Spectra

Figure 11 shows same NMR spectra for various annealing times at 170°C when degradation occurs in air. The ^{13}C solid state NMR spectra show that no degradation induced change of the absorption peaks of methylene or dichloro-carbons for different annealing time, as in Figure 8. However, structural change demonstrates different spectra when degradation occurs in pure oxygen as seen from Figure 12. The absorption peak of the methylene carbon shifts to higher ppm and becomes rougher and smaller compared to that of dichloro carbon with increasing annealing time at the first 40 min. Methylene carbon peak goes back to the original position and become smooth after 50 min. The rough spectra and peak shifting might come from changing polarity after degradation and change of the numbers of methylene and dichloro carbons in the presence of oxygen.

CONCLUSION

Oxygen concentration in purging gas significantly influences the behavior of thermal degradation of PVDC solid. It increases the period of time of each degraded stage. It increases the rate of dehydrochlorination proportionally. The increase of viscosity, due to cross-linking, is also accelerated by oxidation. Activation energy decreases when degradation occurs in pure oxygen

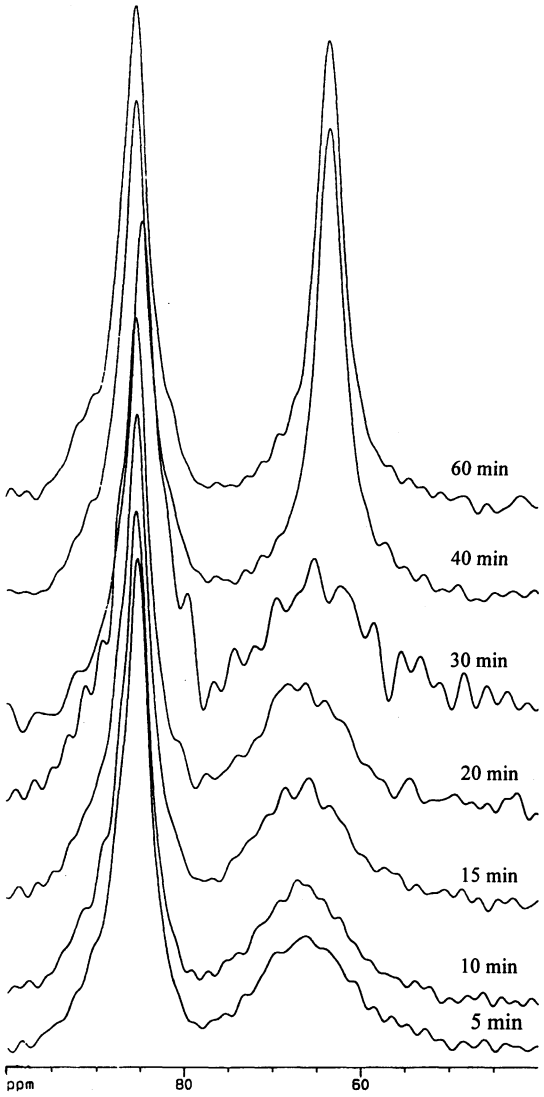

Figure 12. ^{13}C solid-state NMR spectra of methylene group of PVDC annealing for various times at 170°C in pure oxygen.

due to more radicals produced from the cleavage of peroxide groups created during oxidation.

The oxygen can go into the degraded crystalline region through the unzipping dehydrochlorization reaction and subsequent oxidation causes the melting point depression of the crystalline region.

WAXD patterns show a big domain during degradation in pure oxygen. Pure oxygen behaves like a cutter, which can cut the degraded crystalline region into many smaller pieces of crystals, which then remelt and become part of the amorphous region.

The solid-state NMR spectra show no change of PVDC in air at 170°C. In pure oxygen, a polarity change can be found in the earlier stage. The spectra are back to the same position as neat PVDC at later stage.

A thorough vibration spectra study is necessary to understand early stage thermal degradation mechanism of PVDC solid, which will be discussed in a future work.

REFERENCES

1. C. E. Schidknecht, "Vinyl and Related Polymers," John Wiley and Sons, New York, N.Y., 1952, Chapter 8.
2. R. A. Wesseling, "Encyclopedia of Polymer Science and Technology," John Wiley and Sons, New York, N.Y., 1971, Chapter 14, p 540.
3. G. M. Burnett and R. A. Haldon, *Eur. Polym. J.*, **4**, 83 (1968).
4. B. Dolezel, M. Pegoraro, and E. Beati, *Eur. Polym. J.*, **1**, 1411 (1970).
5. R. A. Wesseling, "Polyvinylidene Chloride," John Wiley and Sons, New York, N.Y., 1977, Chapter 9, p 133 and 140.
6. J. N. Hay, *J. Polym. Sci., A-1*, **8**, 1201 (1970).
7. R. D. Bohme and R. A. Wessling, *J. Appl. Polym. Sci.*, **16**, 1761 (1972).
8. G. Montaudo, *J. Polym. Sci.*, **24**, 301 (1986).
9. K. B. Abbas, *J. Appl. Polym. Sci.*, **17**, 3567 (1973).
10. S. E Evsyukov, S. Paasch, and B. Thomas, *Ber. Bunsen-Ges*, **101**, 837 (1997).
11. S. Biniak and J. Siedlewski, *Polym. J. Appl. Chem.*, **36**, 353 (1993).
12. B. A. Howell, A. M. Kelly-Rowley, and P. B. Smith, *Polym. Prepr., Am. Chem. Soc., Div. Polym. Chem.*, **30**, 289 (1989).
13. A. E. Gurgiolo, M. E. Winquist, T. M Knobel, and D. C. Teeters, U.S. Patent 4643953.
14. M. P. Farr and I. R. Harrison, *J. Polym. Sci., Part C, Polym. Lett.*, **24**, 257 (1986).
15. B. A. Howell, *Polym. Prepr., Am. Chem. Soc., Div. Polym. Chem.*, **27**, 439 (1986).
16. Y. S. Chiu, J. Jagur-Grodzinski, and D. J. Vofsi, *J. Polym. Sci., Polym. Chem. Ed.*, **23**, 1193 (1985).
17. J. D. Danforth, *Polym. Prepr., Am. Chem. Soc., Div. Polym. Chem.*, **4**, 163 (1984).
18. J. D. Danforth, *Polym. Prepr., Am. Chem. Soc., Div. Polym. Chem.*, **21**, 140 (1980).
19. A. Ballistrert, S. Foti, G. Mantaudo, and E. Scamporrino, *Polymer*, **22**, 131 (1981).
20. P. Pendleton, B. Vincent, and M. L. Hair, *J. Colloid Interface Sci.*, **80**, 512 (1981).
21. M. Maciejewski, *Polym. J. Macromol. Sci.-Chem.*, **13**, 1175 (1979).
22. D. H. Davies, *J. Chem. Soc., Faraday Trans. 1*, **72**, 2390 (1976).
23. W. Ripperger, W. Oettinger, R. Kaiser, K.Pfitzner, and R. A. Palm,. U.S. Patent 3960768.
24. G. J. Howard, S. Szynaka, and A. L Gatzke, *J. Appl. Polym. Sci.*, **19**, 2633 (1975).
25. D. E. Agostini and A. L. Gatzke, *J. Polym. Sci., Polym. Chem. Ed.*, **11**, 649 (1973).
26. S. S.Barton, P. G. Beswick, and B. H. Harrison, *J. Chem. Soc., Faraday Trans. 1*, **68**, 1647 (1972).
27. D. H. Davies, D. H. Everett, and J. Taylor, *Trans. Faraday Soc.*, **67**, 382 (1971).
28. D. H. Everett and D. J. Taylor, *Trans. Faraday Soc.*, **67**, 402 (1971).
29. G. M . Burnett, R. A. Haldon, and J. N. Hay, *Eur. Polym. J.*, **3**, 449 (1967).
30. Y.-L. In, J.-H. Yang, and M.-H. Wang, *Polymer Testing*, **15**, 525 (1996).
31. W. C. Geddes, *Rubber Chem. and Tech.*, **40**, 177 (1967).
32. G. M. Burnett and R. A. Haldon, *Eur. Polym. J.*, **3**, 449 (1967).
33. K. Matsuo and W. H. Stockmayer, *Macromolecules*, **8**, 660 (1975).
34. T.H. Hsieh and K. S. Ho, *J. Polym. Sci., Part A, Polym. Chem.*, in press.
35. H. Wiener, *J. Polym. Sci.*, **7**, 1 (1951).
36. K. B. Abbas and E. M. Sorvik, *J. Appl. Polym. Sci.*, **17**, 3557 (1973).
37. T.H. Hsieh and K.S. Ho, *J. Polym. Sci., Part A, Polym. Chem.*, in press.
38. B. Wunderlich, "Macromolecular Physics," Vol. I, Academic Press , New York, N.Y., 1973, p 349.